Simulating Microwave-Heated Open Systems: Tuning Competitive Sorption in Zeolites†

Julian E. Santander,‡ W. Curtis Conner, Jr.,§ Hervé Jobic,|| and Scott M. Auerbach*,‡,§

Department of Chemistry, University of Massachusetts, Amherst, Massachusetts 01003, Department of Chemical Engineering, University of Massachusetts, Amherst, Massachusetts 01003, and Institut de Recherches sur la Catalyse, Ecole Normale Superiore de Lyon, France

Received: March 31, 2009; Revised Manuscript Received: May 20, 2009

We have developed a new grand canonical molecular dynamics (GCMD) algorithm to study microwave (MW) heating effects on competitive mixture sorption and have applied the method to methanol and benzene in silicalite zeolite. The new algorithm combines MW-driven molecular dynamics with grand canonical Monte Carlo (GCMC), the latter modeling adsorption/desorption processes. We established the validity of the new algorithm by benchmarking single-component isotherms for methanol and benzene in silicalite against those obtained from standard GCMC, as well as against experimental data. We simulated single-component and mixture adsorption isobars for conventional and MW-heated systems. In the case of the single-component isobars, we found that for dipolar methanol, both the MW and conventional heated isobars show similar desorption behavior, displaying comparable loadings as a function of molecular temperature. In contrast, nonpolar benzene showed no desorption upon exposure to MWs, even for relatively high field strengths. In the case of methanol/benzene mixtures, the fact that benzene is transparent to the MW field allows the selective desorption of methanol, giving rise to loading ratios not reachable through conventional heating.

1. Introduction

Microwave (MW) heating has provided a wealth of interesting phenomena and important applications in materials science.[1] Once relegated to organic synthesis only, MWs are now impacting the synthesis of zeolites and other oxides,[2] the use of heterogeneous catalysts,[3] and competitive adsorption in zeolites.[4,5] For example, Turner et al.[4] found that sorption selectivities of mixtures in zeolites could be reversed with MW fields, and Vallee et al.[5] found that MW-heated zeolite-guest systems can be understood in terms of effective "surface temperatures" controlled by MW field properties. Although these MW effects appear to be real, their microscopic interpretation is far from clear. In the present article, we report a new open-system, MW-driven molecular simulation method to shed light on the distributions of energy and matter present in MW-heated zeolite−guest systems.

To investigate the energy distributions present in MW-heated steady-state systems, we have reported a series of MW-driven molecular dynamics studies on methanol and benzene in all-silica FAU and MFI zeolites to explore how energy distributions and diffusion can be influenced by MW energy.[6−8] We predicted that MW-heated mixtures can be characterized by a collection of steady-state temperatures: one for the zeolite and another for each adsorbed guest phase.[6] Regarding mixture diffusion, this gives a picture of different guest phases diffusing as if they were at equilibrium—each guest phase with its own temperature.[6] Regarding competitive sorption, we suggested that nonequilibrium energy distributions could be used to tune sorption selectivities, but since all our previous simulations were at constant guest loading, our suggestions remained "educated guesses."

Modeling adsorption/desorption equilibria is usually accomplished with the grand canonical Monte Carlo (GCMC) algorithm,[9] involving random insertion/deletion attempts controlled by the potential energy distribution of adsorbed molecules and the chemical potential of an external particle reservoir. A direct GCMC simulation of MW-driven sorption is complicated by the fact that MW energy carries an inherent dynamics, while Monte Carlo simulations (typically) lack a system clock.[10] To model MW-driven sorption, we imagine marrying MW-driven molecular dynamics with grand canonical insertion/deletion moves. Such a "GCMD" approach has been reported for modeling gradient-driven diffusion in zeolites through the use of control volumes under periodic boundary conditions.[11] GCMD has also been used for modeling the origin of hysteresis in adsorption.[12] In these cases, the intent was to model an inherently dynamical process under equilibrium, thermodynamic control. In the present article, we have an altogether different objective.

We seek to model a thermodynamic process (adsorption/desorption) in a MW-driven, nonequilibrium system. In the present work, we are less interested in the dynamics of adsorption/desorption, which is ultimately controlled by diffusion. Instead, we simulate dynamics as a mechanism for introducing MW energy into the system. Such energy pushes and pulls on adsorbed guest molecules, especially if they are polar, eventually exciting their zeolite-guest potential energy distribution. It is precisely this distribution that GCMC relies upon for producing fluctuations in guest loading. We thus suggest a mechanism for MW-driven sorption to be explored by the detailed simulations discussed below. In the end, we predict that benzene in silicalite is transparent to MW radiation because it is largely nonpolar,[5,6] while methanol can be completely desorbed with a strong enough field. These facts

† Part of the "H. Ted Davis Special Section".

* To whom correspondence should be addressed. E-mail: auerbach@chem.umass.edu.
‡ Department of Chemistry, University of Massachusetts.
§ Department of Chemical Engineering, University of Massachusetts.
|| Ecole Normale Superiore de Lyon.

10.1021/jp902946g CCC: $40.75
Published on Web 06/17/2009

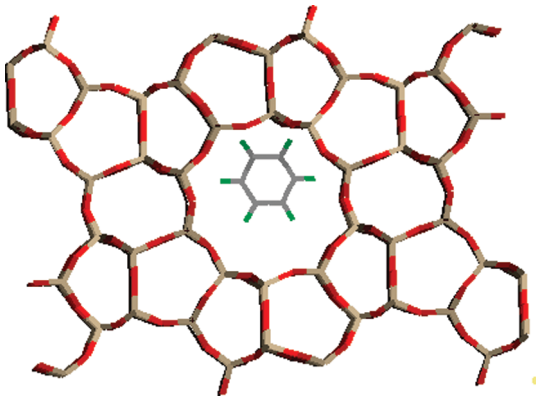

Figure 1. Silicalite structure. The straight channels observed in the image constitute one of the distinct adsorption sites for benzene.

allow the sorption selectivity to be tuned by MWs in ways that conventional heating cannot achieve.

The remainder of this article is organized as follows. in Section 2 we discuss our GCMD simulation approach and the force field applied to model methanol/benzene in silicalite; in Section 3 we discuss the results of single-component and mixture sorption simulations; and in Section 4 we offer concluding remarks.

2. Methodology

This section discusses the algorithm developed to simulate competitive adsorption using the GCMC technique for insertions and deletions of guest molecules while modeling the interaction of the zeolite-guest system with an external MW field using a MD simulation. Both simulation techniques have been discussed in detail by previous authors.[8,9,13,14] Here, we detail our implementation of both methods simultaneously augmented by an external MW field. This MW driven GCMD algorithm was applied to the single component and competitive adsorption of benzene and methanol in the zeolite silicalite.

2.a. Zeolite Framework. All adsorption simulations were performed on silicalite (all-silica MFI structure),[1,15] which provides a useful model system[1] for the industrial catalyst HZSM-5. To build a simulation cell of sufficiently large size for an acceptable short-range potential energy cutoff, we simulated two silicalite unit cells in the *c* direction, giving a total 576 zeolite atoms. This simulation cell contains eight channel segments with approximate diameters of 5.5 Å, and eight intersection spaces (connecting channel segments) of about 8.7 Å in diameter.[13] A portion of this framework structure is shown schematically in Figure 1.

2.b. Potential Energy Surface. The potential energy model used for these simulations is the same one reported by Blanco and Auerbach.[6] In the present paper we will not describe this potential function in detail; instead we give a brief description of its key components. The potential energy function has the following general form:

$$V = V_Z + V_G + V_{ZG} + V_{GG}$$

Here, V_Z and V_G treat the zeolite and guest intramolecular vibrations, while V_{ZG} handles zeolite−guest interactions, and V_{GG} controls the intermolecular guest interactions including those for binary mixtures. Short-range zeolite intramolecular interactions were described using a Buckingham (exp−6) force field, while host−guest and guest−guest intermolecular energies were modeled as a Lennard−Jones (12-6) fluid. Snurr et al.[13,14] showed that this type of force field reproduces experimental adsorption data, via GCMC simulations. Moreover, Blanco and Auerbach[6−8] used this approach to simulate the effects of heating different zeolite−guest systems using a MW field as a heat source. Long-range Coulombic forces were simulated using fixed atomic point charges evaluated using Ewald summations.[9] The fixed point-charge approximation is acceptable for simulating MW heating because MW frequencies are too low to distort atomic charge distributions.

2.c. GCMC. We performed standard GCMC simulations of methanol, benzene, and mixtures in silicalite to test the equilibrium GCMD simulations, discussed below. The GCMC method applied in this work follows the Monte Carlo acceptance rules found in Appendix F of Frenkel and Smit.[9] In the grand canonical ensemble, the control variables are μ, V, and T, where μ is the chemical potential of the ideal gas in "contact" with the zeolite, V is the volume of our simulation cell, and T is the temperature. To facilitate guest molecule insertions, we used the insertion bias found in refs 16 and 17. This bias algorithm attempts insertions more frequently in the most energetically favored adsorption sites; these sites we identified using a probe particle, 0.3 Å in size, to map the potential energy surface. During normal GCMC simulations the framework and shape of the inserted molecules was kept fixed, although, during insertions the orientation of the guest molecule was randomized. Averages were calculated using the last 10^6 steps of the simulations. All simulations ran for a total of 2×10^6 Monte Carlo steps and completed in 30−40 h of CPU time on a 3.0 GHz Intel processor with 1 GB of RAM.

2.d. Molecular Dynamics. The algorithm used to perform the MD portions of the GCMD simulations is the same one described by Blanco and Auerbach,[6] involving the following equations of motion:

$$\frac{\mathrm{d}\vec{r}_i}{\mathrm{d}t} = \frac{\vec{p}_i}{m_i} \qquad \frac{\mathrm{d}\vec{p}_i}{\mathrm{d}t} = -\frac{\partial V}{\partial r_i} + q_i \vec{E}_t$$

Here r_i and p_i represent the position and momentum of each particle in phase space, $V(r)$ is the potential function described above, and q_iE_t represents the force experienced by each particle due to the presence of the MW field. The MW electric field attempts to pull charged particles depending on the sign of charge and the phase of the field. When these charges are covalently bound as in methanol, the effect of the field is to align the molecular dipole with the field orientation. Such alignment pulls molecules away from their preferred host−guest configuration, thereby adding host−guest potential energy to the system. This energy spreads into guest center-of-mass potential and kinetic energy, thereby activating molecular desorption. To simulate these effects we employed the velocity Verlet integration algorithm[9] with a time step of 1 fs, which was sufficient to maintain stable dynamics even with strong MW fields. All the simulations reported in this paper were performed using the program DIZZY.[18]

To balance the effect of MW heating, we employed the Andersen thermostat[19] as in our previous studies,[6−8] to simulate the steady states produced in experiments on MW heating.[4,5] This thermostat replaces the velocity of a random particle with a velocity taken from the appropriate Maxwell−Boltzmann distribution with an average replacement frequency. In our MW-driven simulations, replacements were carried out every 10 MD

steps on average, and the number of particles substituted each time was set to one. We have shown in previous work that this thermostat produces the same steady-state MW-driven energy distributions as those obtained from an explicit helium bath gas.[20] For the simulation of the MW field, we assumed a monochromatic field along the z axis as given by Blanco:[6] $E(t) = E_0 \sin(\omega t)$, where ω and E_0 represent the field frequency and strength, respectively. In order to observe MW effects in a molecular simulation time scale (~ns), we set our field parameters to $\omega = 9.4 \times 10^{11}$ Hz, in the blue end of the MW spectrum, and $E_0 = 0-1.5$ V/Å, a relatively high field strength. Because silicalite exhibits structural anisotropy along x, y, and z axes, it is interesting to explore how MW effects may differ for fields pointing in different directions. We will also consider the effect of using different MW frequencies on the energy transfer dynamics. We report on these issues in a forthcoming publication.

2.e. GCMD. The idea behind our implementation of the GCMD algorithm is to use the MW-driven MD to introduce energy into the zeolite-guest system, particularly into the zeolite−guest potential energy. These MW-driven MD segments are interspersed with GCMC runs, which respond to the excited state of the system through guest insertions/deletions (typically more deletions), hence producing MW-driven desorption. Care has to be taken to balance the lengths of the MD and MC segments. If the ratio of run lengths MC/MD is too large, the potential energy distribution will essentially equilibrate, hence nullifying the effect of the MW field. Conversely, if the ratio MC/MD is too small, there will be insufficient attempts at insertion/deletions, and again the effect of the MW field will not be seen. We find stable results with a MC/MD ratio of ~100/1000.

Previous implementations of GCMD have been used to simulate gradient-driven diffusion, requiring several control volumes to represent high- and low-density regions.[11] In these previous studies, GCMC is carried out in control volumes only, and many GCMC steps are typically required to maintain "chemical equilibrium" in these volumes. Our goals and implementation differ significantly from those of previous GCMD studies. In the present study, we are primarily interested in MW-driven *desorption*, and as such, we do not track diffusion processes. As with standard GCMC, our focus on an ostensibly thermodynamic property allows us to make GCMC insertions/deletions directly in the central simulation cell, without any control volume.

Here, we discuss how we have blended the properties and fluctuations of GCMC and MD. All our MD simulations allow full framework and guest-molecule flexibility—this is crucial for the dynamical stability of MW-driven MD simulations—while GCMC simulations typically hold the framework fixed, and sometimes even hold guest-molecule shapes fixed as well. We have found it important for the stability of our GCMD approach to blend similar fluctuations in the MD and GC segments. To achieve this, each GCMC segment keeps the zeolite framework fixed at the structure produced in the most recent MD step. As such, the GCMC samples insertions/deletions into different framework structures from one GCMC segment to the next.

To sample an equilibrium distribution of intramolecular shapes during attempted GCMC insertions, we generate a library of such shapes before performing GCMD. We ran short MD simulations (10 ps) of a dense fluid of guests without zeolite, set at the target temperature of the GCMD run with the Andersen thermostat. These simulations were run in a cell mimicking that of silicalite (dimensions $20 \times 20 \times 26$ Å^3), typically containing 30 or more molecules. Atomic coordinates were written to disk every 0.1 ps, creating a library of ~3000 molecular shapes. The initial condition for this guest fluid was generated by standard GCMC insertions into an empty box with pressure set to 1000 atm. A molecular shape library was generated for every GCMD temperature, and for each type of guest molecules.

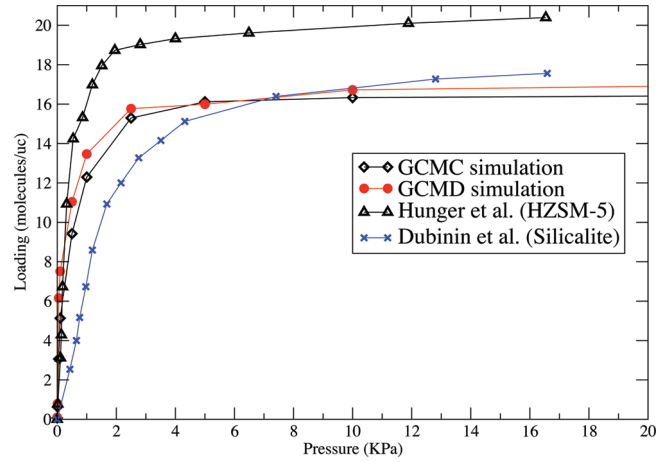

Figure 2. Adsorption isotherm for methanol in silicalite, comparing GCMC (diamonds) and GCMD (circles) simulation results at 300 K with experiments. At saturation, both simulation algorithms match Dubinin et al. (crosses) for silicalite.

Each GCMD simulation is initialized by running a short MD simulation of ~1 ps (1000 steps). In the final step of this run, all atomic positions and velocities are stored. At this point, the algorithm performs a GCMC simulation beginning with the zeolite and guest positions given by the last MD step. Guest insertions are attempted from the library of molecular shapes. If insertions are accepted, new guest-atom velocities are also initialized in preparation for the next MD segment. As discussed above, after ~100 GCMC steps, the algorithm returns to ~1000 steps of MD. At the final step of this MD segment, positions and velocities are stored in preparation for the next GCMC segment, and so on. The algorithm continues to alternate MD and GCMC segments until sufficient statistics for guest loading are gathered. We found that 300 000 GCMC steps were sufficient to converge guest-loading statistics.

In closing, we note that in principle our algorithm requires two input temperatures: the GCMC Metropolis acceptance criterion temperature, and the Andersen MD thermostat temperature. In general, these were set to the same value, defining the overall GCMD temperature.

3. Results

In this section, we show results of standard GCMC and our GCMD, to establish the validity of our new sampling method. We also compare with experiments to test our force field model. We show below single-component equilibrium isotherms, single-component isobars under thermal and MW heating, and binary mixture isobars also under thermal and MW heating.

3.a. Adsoprtion Isotherms of Methanol and Benzene in Silicalite. Single-component isotherms of methanol and benzene were computed to benchmark the force field and to confirm the validity of the GCMD algorithm. Various different simulation runs were made in order to generate the methanol isotherm in silicalite at 300 K. The results obtained (Figure 2) show very good agreement between GCMC and GCMD. We obtain a higher saturation loading and a steeper slope for the GCMD isotherm when compared to the GCMC results. This is due to

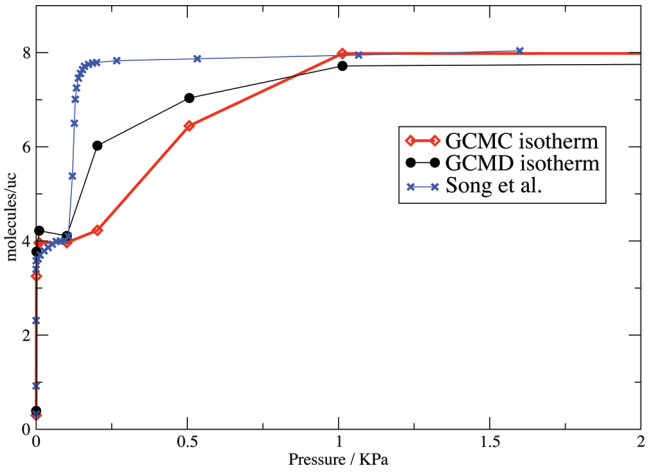

Figure 3. Adsorption isotherm for benzene in silicalite, comparing GCMC (diamonds) and GCMD (circles) simulation results at 300 K with experiment by Song et al. The GCMD (circles) data show better agreement with Song et al. in the regime corresponding to the filling of channel adsorption sites ($P = 0.13-1$ KPa).

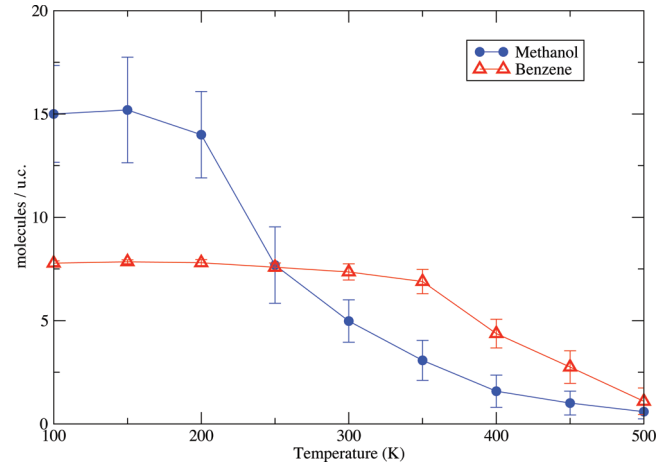

Figure 4. Single-component adsorption isobars of methanol and benzene in silicalite ($P = 10$ KPa).

the fact that the GCMD method permits the zeolite and guest molecules to distort their shapes during MD in-between MC steps, simulating framework fluctuations and intramolecular guest vibrations. The end result is that the GCMD algorithm gives a better approximation to what really happens during the adsorption process. Both GCMD and GCMC agree well with the data of Hunger et al.[21] for methanol in HZSM-5 in the Henry's law region, which is surprising because HZSM-5 contains selective adsorption sites. Perhaps more important is that our simulation data agrees quite well with the saturation loadings of Dubinin et al.[22] for methanol in silicalite. Reproducing saturation properties is paramount for the present study because we wish to model MW driven desorption for binary mixtures near their saturation loadings.

Figure 3 shows the GCMC and GCMD generated isotherms for benzene in silicalite alongside the experimental data of Song et al.,[23] all at 300 K. Both the GCMD and GCMC methods found two distinct adsorption sites within the framework. The first site, which fills at lower pressures, locates benzene in the intersections connecting the straight and zigzag channels of silicate, allowing a loading of 4 molecules per unit cell. In this region of the isotherm a pseudosaturation point is reached, and both simulation methods give almost identical results with the data of Song et al. up to pressures of ~0.13 KPa. In the region between 0.13 and 1 KPa, GCMC, GCMD, and experiment show systematic discrepancies. In this regime benzene begins filling the channel sites in silicalite (see Figure 1), which is a relatively tight fit compared to the intersection sites. The data of Song et al. shoot right up to the saturation loading of 8 molecules per unit cell at $P \approx 0.13$ KPa, while at 0.24 KPa GCMD achieves 6 molecules per cell and GCMC is stuck at 4 molecules per cell. This discrepancy can be understood as follows. Both GCMC and GCMD fix the simulation cell volume by holding the unit cell parameters at their experimental X-ray values. In addition to this constraint, the GCMC simulations maintain a fixed framework structure, while GCMD allows framework fluctuations (at constant volume) during the MD segments. As such, GCMC requires relatively high pressures to fill the fixed channel sites, while GCMD fills the same sites more easily (at lower pressures) because of framework fluctuations. The experimental data involve none of these constraints (except for fixed pressure), allowing unit cell shape/volume fluctuations that facilitate saturation at quite low pressures. Above pressures of 1 KPa, all isotherms show a very specific loading of 8 benzenes per unit cell, represented by 4 molecules in the intersection sites, and 4 molecules in the channels sites.

Although our simulated isotherms do not show perfect agreement with experiment, they show the qualitative features needed to learn about *competitive adsorption near saturation* under MW heating, as discussed below. In what follows, we focus on showing the GCMD results, having demonstrated the validity of its sampling through comparison with standard GCMC.

3.b. Adsorption Isobars. To benchmark the extent to which MW heating produces desorption in zeolite-guest systems, we computed equilibrium isobars for single-components methanol and benzene in silicalite, and for the mixture. The control variable for the equilibrium isobars is temperature, while that for the MW heated isobars is MW field strength. A pressure of 10 KPa was chosen, since it was found from the isotherms that both methanol and benzene isobars range from saturation to complete desorption within the temperature range of 100−600 K.

The single-component isobars shown in Figure 4 indicate that benzene desorption occurs at higher temperatures than for methanol, which is explained by benzene's higher heat of adsorption. Indeed, our simulations give the following (constant volume, infinite dilution) heats in silicalite: benzene (intersection) = 59.2 kJ/mol; benzene (channel) = 54.7 kJ/mol; methanol = 35.3 kJ/mol. These results agree reasonably well with the data of Pope et al.,[24,25] which are benzene (intersection) = 54 kJ/mol; benzene (channel) = 60−74 kJ/mol; methanol = 45 kJ/mol. Although our simulations do not reproduce the order of benzene intersection and channel site energies, they do reproduce the higher benzene heats of adsorption relative to methanol. Given these heats of adsorption and the fact that two methanol molecules occupy roughly the same volume as one benzene molecule, we expect the multicomponent adsorption system to exhibit a mixture of methanol and benzene at low temperatures, where benzene would occupy the intersections and methanol the channels.

In Figure 5 we show the equilibrium mixture isobar simulated with GCMD, obtained by "exposing" the zeolite to an equimolar gas of benzene and methanol. Figure 5 shows that, from 100 to 300 K as methanol is thermally desorbed, benzene loading increases to fill the voids left by methanol desorption. Upon further heating above 300 K, benzene begins its thermal desorption. We note that heating produces a switch in adsorption

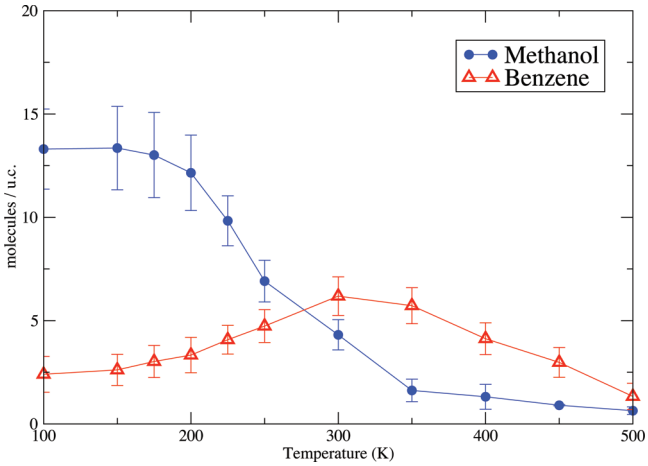

Figure 5. Multicomponent adsorption isobar of methanol and benzene in silicalite ($P_{benzene} = P_{methanol} = 5$ KPa). The maximum in benzene loading around 300 K is a multicomponent effect.

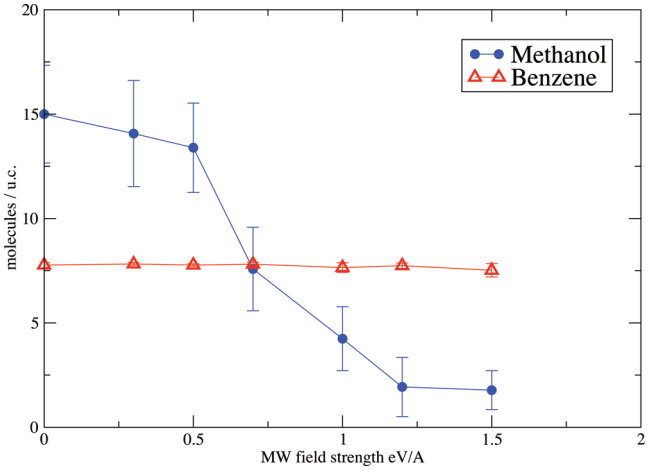

Figure 6. Methanol (circles) and benzene (triangles) single-component isobars at 10 KPa. The thermostat was set at 100 K with heating produced by a MW field of varying field strength.

selectivity. Indeed, at 100 K, the methanol/benzene loading ratio is 13.0/2.5 ~ 5, while at 350 K the same ratio becomes 2.0/6.0 ~ 0.3. We now turn to exploring the same effect under conditions of MW heating, beginning with the single-component isobars and ending with the mixture isobar.

For the simulation of the MW-heated systems, the Andersen thermostat (MD) and the gas phase (GCMD) temperatures were both set to 100 K, consistent with the minimum temperature in Figures 4 and 5. The zeolite−guest system was exposed to a MW field discussed above with field strengths in the range 0.3−1.5 V/Å, keeping the Andersen thermostat replacement period at 1 particle per 10 fs on average.

Figure 6 shows the single-component MW heated isobars. For methanol, the conventional-heated and MW-heated isobars show qualitatively similar forms because the dipolar nature of methanol makes it a strong MW absorber. On the other hand, the benzene MW-driven isobar (Figure 6) and the conventional-heated isobar (Figure 4) show different behavior because nonpolar benzene is essentially transparent to the MW field, which leaves the MW-driven loadings unchanged from their saturation value. Only at very high MW field strength does benzene begin to show some heating, induced by torsional vibrations that lead to small dipole moments.

To explore the origin of the MW-driven desorption of methanol shown in Figure 6, we extracted steady-state, center-

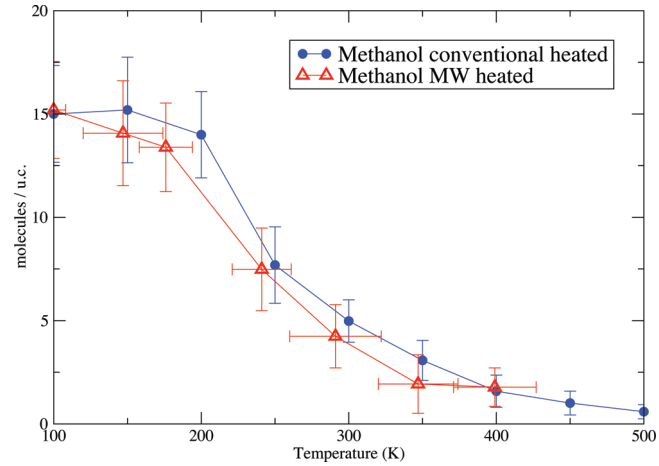

Figure 7. Methanol adsorption in silicalite comparing conventional-heating (circles) and MW-heating (triangles) GCMD results. For the MW-heated system, the temperature is extracted from the steady state, center-of-mass kinetic energy of adsorbed methanol.

TABLE 1: Methanol Center-of-Mass Temperature and Total System Temperature As Functions of MW Field Strength, with an Andersen Thermostat Set to 100 K

E field (V/Å)	MeOH temp (K)	system temp (K)	MeOH loading/u.c.
0.3	147 ± 27	102 ± 10	14.1 ± 2.5
0.5	176 ± 18	103 ± 9	13.4 ± 2.1
0.7	241 ± 20	109 ± 16	7.6 ± 2.0
1.0	291 ± 31	143 ± 11	4.2 ± 1.5
1.2	347 ± 27	190 ± 21	1.9 ± 1.4
1.5	399 ± 28	231 ± 21	1.8 ± 0.9

of-mass temperatures of methanol during MW-driven GCMD simulations. Instead of plotting methanol loading vs MW field strength as in Figure 6, we plot in Figure 7 methanol loading vs MW-heated temperature, alongside the isobar from conventional heating. The striking coincidence of these curves indicates that the effective center-of-mass methanol temperature is a quantitative predictor of MW-heated desorption. Table 1 shows this effect as well, including also the total system temperature which is dominated by the zeolite degrees of freedom. Since the all-silica zeolite is largely transparent to MWs, the total system temperature is much lower than the effective methanol temperature. These results suggest that the methanol loading is controlled by the MW field and is relatively impervious to the zeolite bath temperature.

The methanol and benzene mixture isobar with MW heating is shown in Figure 8. This shows the remarkable prediction that only methanol desorbs from the MW field, leaving benzene to take its place even at the highest field strengths. Like the conventionally heated system, this shows a switch of selectivity with MW field strength. However, the switch is *virtually complete*, going from 13.0/2.5 in favor of methanol with no MW field, to 2.0/8.0 in favor of benzene at high fields. The selectivity for benzene could, in principle, be even greater at higher field strengths. This result suggests new ways to tune mixture adsorption selectivities for zeolite-guest systems, by accessing MW-driven steady states that are not reachable at equilibrium.

Concluding Remarks

We have developed a new GCMD algorithm to study MW heating effects on competitive mixture sorption, and have applied the method to methanol and benzene in silicalite zeolite. The new algorithm combines MW-driven molecular dynamics

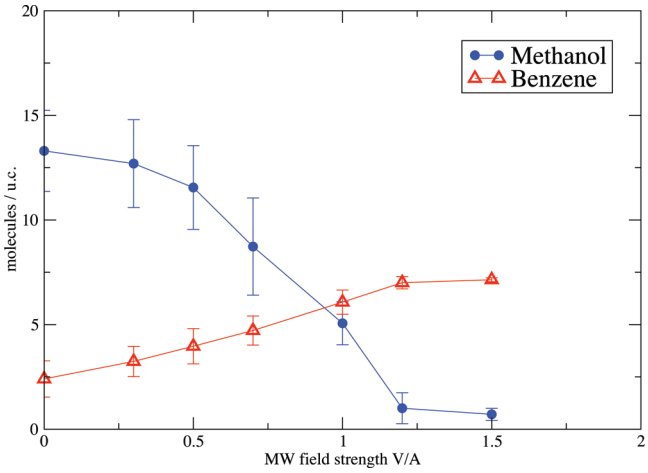

Figure 8. Methanol (circles) and benzene (triangles) mixture isobar in silicalite at 10 KPa (equimolar gas). The thermostat was set at 100 K with heating produced by a MW field of varying strength. Only methanol absorbs enough MW energy to desorb from the framework.

with GCMC, the latter modeling adsorption/desorption processes. To sample intramolecular vibrations during GCMC, we have generated libraries of molecular shapes from thermostatted molecular dynamics of bulk fluids. We established the validity of the new algorithm by benchmarking single-component isotherms for methanol and benzene in silicalite against those obtained from standard GCMC, as well as against experimental data. In general, we find excellent agreement between standard GCMC and our new GCMD algorithm for equilibrium systems, with GCMD actually providing a more realistic treatment of zeolite and guest-molecule vibrations.

We simulated single-component and mixture adsorption isobars for conventional and MW-heated systems. In the case of the single component isobars, we found that for dipolar methanol, both the MW and conventional heated isobars show similar desorption behavior, displaying comparable loadings as a function of molecular temperature extracted from center-of-mass kinetic energy. This shows that the center-of-mass temperature is a quantitative predictor of sorption in equilibrium and MW-driven zeolite-guest systems.

In contrast, nonpolar benzene showed no desorption upon exposure to MWs, even for relatively high field strengths. In the case of methanol/benzene mixtures, the fact that benzene is transparent to the MW field allows the selective desorption of methanol, giving rise to loading ratios not reachable through conventional heating. This suggests the possibility of tuning sorption selectivities with MW radiation for MW-based separations, and in general, producing selective heating with MW energy. Much work needs to be done before this becomes a reality, including understanding MW-driven diffusion in anisotropic zeolites, optimizing selectivities with variable frequency MW fields, and testing all these predictions with in situ spectroscopic probes of MW heated systems.

Acknowledgment. We thank Mr. Aldo Combariza and Prof. Cristian Blanco for their helpful contributions in the development of the DIZZY software. We also acknowledge generous funding from the National Science Foundation (NSF 0553577; Dr. John Regalbuto). Finally, we thank Mr. Karl Hammond for stimulating discussions on zeolite adsorption.

References and Notes

(1) Auerbach S. M., Carrado K. A., Dutta P. K., Eds. *Handbook of Zeolite Science and Technology*; Marcel Dekker: New York, 2003.
(2) Tompset, G. A.; Conner, W. C.; Yngvensson, K. S. *Chem. Phys. Chem.* **2006**, *7*, 296.
(3) Marun, C.; Conde, L. D.; Siub, L. S. *J. Phys. Chem.* **1999**, *103*, 4332.
(4) Turner, M. D.; Laurence, R. L.; Conner, W. C.; Yngvensson, K. S. *J. AIche* **2000**, *46*, 758.
(5) Vallee, S. J.; Conner, W. C. *J. Phys. Chem. C* **2000**, *112*, 15483.
(6) Blanco, C.; Auerbach, S. M. *J. Phys. Chem. B* **2003**, *107*, 2490.
(7) Blanco, C.; Auerbach, S. M. *J. Am. Chem. Soc.* **2002**, *124*, 6250.
(8) Blanco, C.; Auerbach, S. M. *J. Comput. Theor. Nanosci.* **2004**, *1*, 180.
(9) Frenkel D., Smit B. *Understanding Molecular Simulations: From Algorithms to Applications*; Academic Press: San Diego, 1996.
(10) Saravanan, C.; Auerbach, S. M. *J. Chem. Phys.* **1997**, *107*, 8132.
(11) Arya, G.; Chang, H. C.; Maginn, E. J. *J. Chem. Phys.* **2001**, *115*, 8112.
(12) Sarkisov, L.; Monson, P. A. *Langmuir* **2000**, *16*, 9857.
(13) Gupta, A.; Clark, L. A.; Snurr, R. Q. *Langmuir* **2003**, *16*, 3910.
(14) Snurr, R. Q.; Bell, A. T.; Theodorou, D. N. *J. Phys. Chem.* **1994**, *98*, 5111.
(15) International Zeolite Association, Database of zeolite structures, http://www.iza-structure.org/databases.
(16) Snurr, R. Q.; Bell, A. T.; Theodorou, D. N. *J. Phys. Chem.* **1993**, *97*, 13742.
(17) Allen M. P., Tildesley D. J. *Computer Simulation of Liquids*; Clarendon Press: Oxford, 1987.
(18) Henson, N. J. Ph.D. Thesis, Oxford University, Oxford, 1996.
(19) Andersen, H. C. *J. Chem. Phys.* **1980**, *72*, 2384.
(20) Combariza, A. F.; Sullivan, E.; Auerbach, S. M. *Eur. Phy. J. Special Top.* **2007**, *141*, 93.
(21) Hunger, B.; Matysik, S.; Heuchel, M.; Einicke, W. D. *Langmuir* **1997**, *13*, 6249.
(22) Dubinin, M. M.; Rakhmatkariev, G. U.; Isirikyan, A. A. *Izv. Akad. Nauk. SSSR, Ser. Khim.* **1990**, 1950–1950 (English translation, originally submitted in 1988).
(23) Song, L.; Sun, Z.; Duan, L.; Gui, J.; McDougall, H. S. *Microporous Mesoporous Mater.* **2007**, *104*, 115.
(24) Pope, C. G. *J. Chem. Soc.−Faraday Trans.* **1993**, *89*, 1139.
(25) Pope, C. G. *J. Phys. Chem.* **1986**, *90*, 835.

JP902946G